

Correlation aspects between morphology, infrared and acoustic absorptions properties of various materials

O. VASILE*, F. MICULESCU, S. I. VOICU

University Politehnica of Bucharest, 313 Splaiul Independentei, Bucharest, 060042, Romania

Currently, on the global civil engineering, materials for walls, floors, ceilings from inside of residential buildings are selected according to the shape, color and sound absorption characteristics. This paper presents the results of complex analysis in terms of microscopic, chemical and acoustic properties for six types of materials based on polyurethane and wood. Before presenting the results of absorption-reflection acoustic characteristics a brief theoretical aspect of the transfer function method are show. With this new approach of combined analysis, the correlation can be made between: materials porosity by microscopic study, chemical composition by the FT-IR method and absorption-reflection characteristics of acoustic interferometer analysis.

(Received January 12, 2012; accepted June 6, 2012)

Keywords: Morphology, Infrared absorption, Acoustic absorption, Materials properties

1. Introduction

Usually, in scientific literature, the study of various types of materials is done through different methods of testing and different characteristics are studied: microscopic [1,2], chemical [3-5] or acoustic [6-8]. This paper presents a complex analysis in terms of microscopic, chemical and acoustic analysis for six types of materials. Also, try to find some common characteristic features so we can have a complete and unified characteristic of a type of material, in terms of physico-chemical aspects.

In this study were analyzed commercial samples of polyurethane materials and wood. Sample 1 is composed of a mixture of cork and sample 6 is composed of a mixture of sawdust (see Fig. 1 a, f). Samples from 2 to 5 are various forms of commercial of polyurethane, usually used for floor or wall insulation (see Fig. 1 b-e).

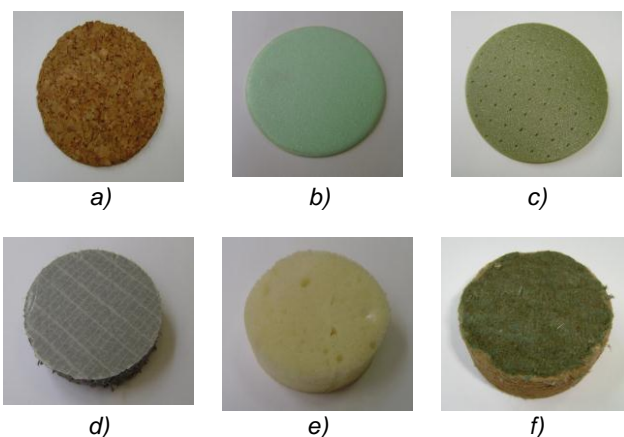


Fig. 1. Photos of the 6 samples (a...f corresponds to 1...6 samples).

The main purpose of the paper is the comparative analysis of absorption and reflection characteristics for

various types of porous structures taking into account the microscopic analysis and chemical composition of materials made by FT-IR analysis.

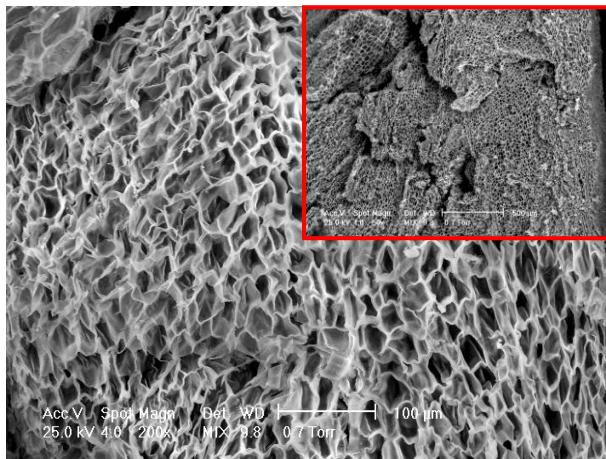
After a imagistic analysis, on the following chapters of this paper and the FT-IR analysis in the absorption and reflection coefficient study, have started a brief theoretical overview of the problem then, is presented the concrete results of the experimental samples.

2. Scanning electron microscopy analysis

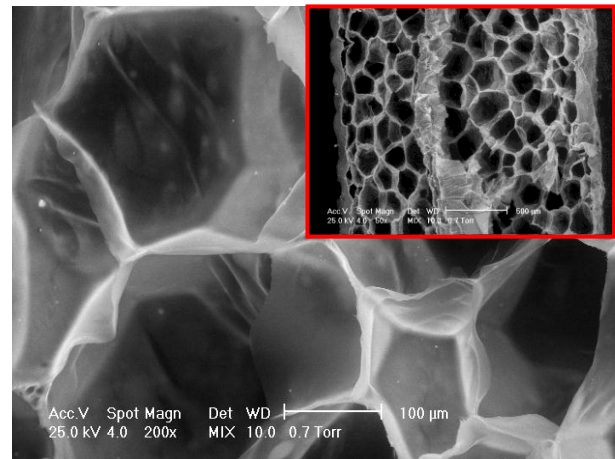
For analysis by SEM microscopy the samples were examined in a scanning electron microscope (Philips XL 30 ESEM TMP) equipped with secondary electron detector in low-vacuum and solid state detector with two diodes BSE. The microscopy operating conditions were as follows: 0° tilt angle, 35° TOA, 25kV accelerating voltage, spot size equal with 4 and 10 mm working distance.

The obtained signals were a mixing between secondary and backscattered electrons, for morpho-compositional results. Samples were mounted on aluminum substrates coated with double adhesive carbon tape and subsequently analyzed. Due to special performance of the microscope, in neither case was necessary to cover the samples with conductive material.

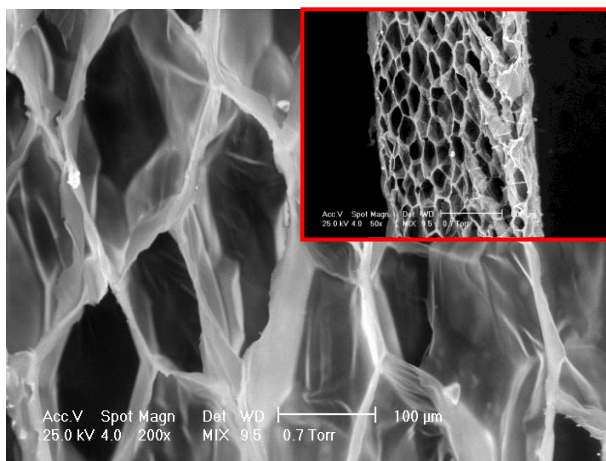
Samples were analyzed in cross section after mechanical cutting with surgical scalpel and sample thickness was measured in advance.



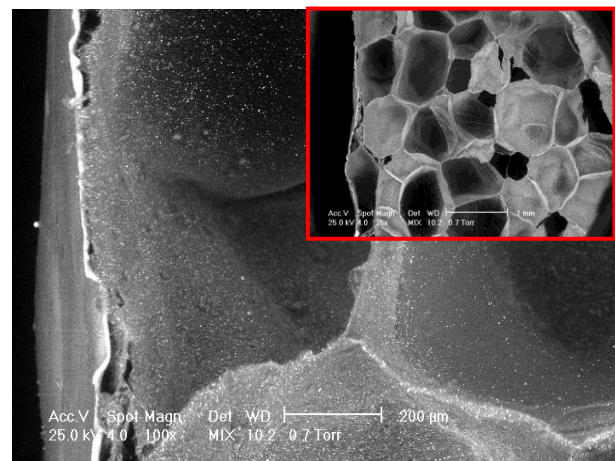
a) Sample 1



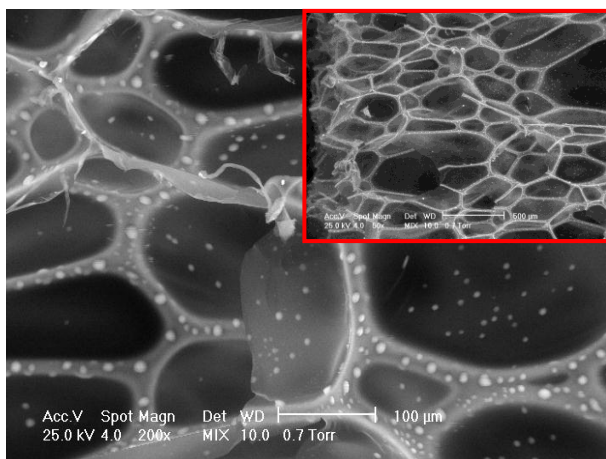
b) Sample 2



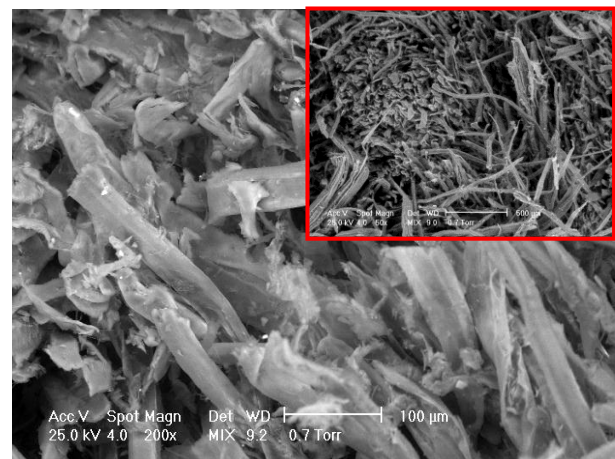
c) Sample 3



d) Sample 4



e) Sample 5



f) Sample 6

Fig. 2. SEM micrographs of analyzed samples.

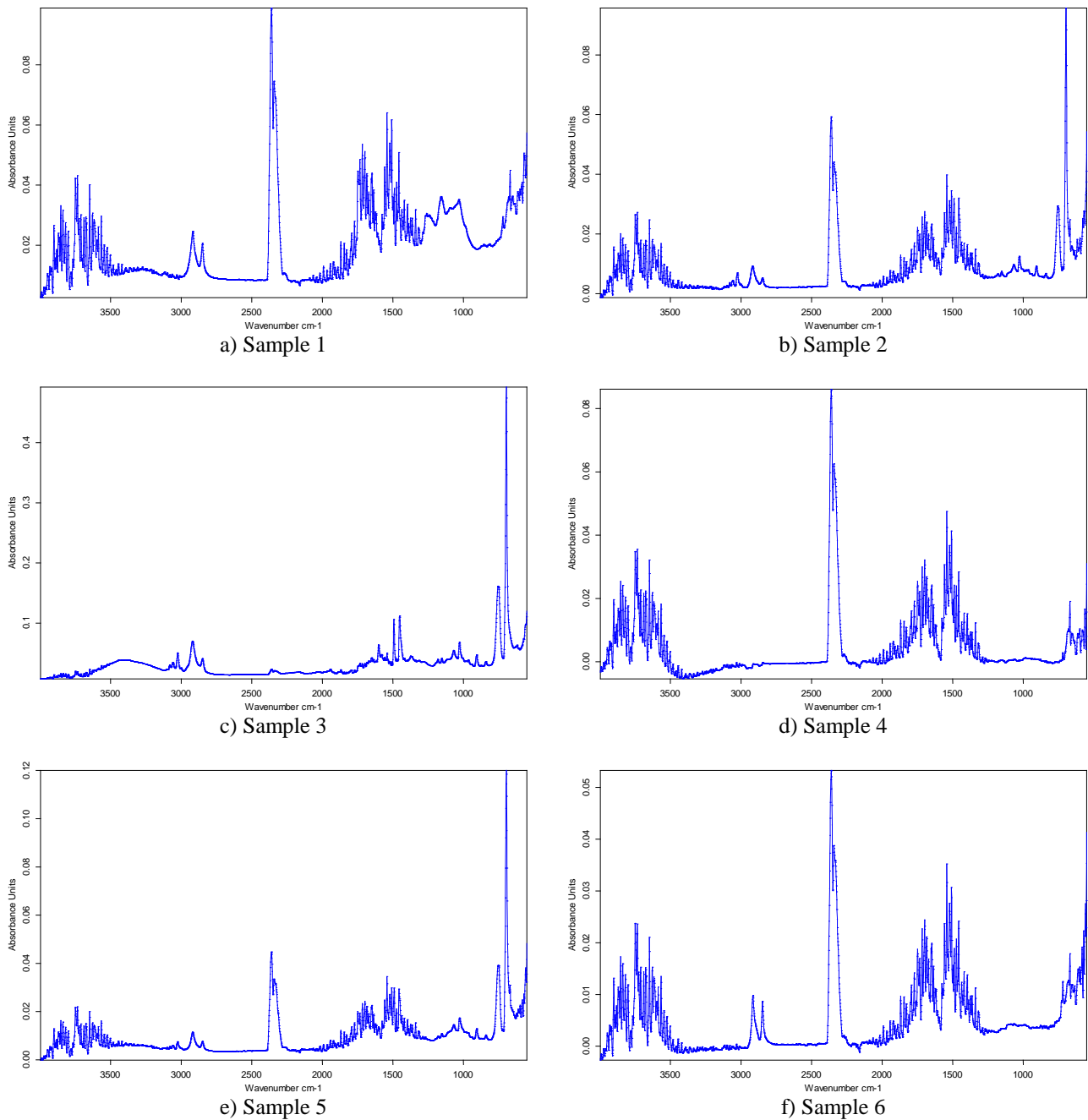


Fig. 3. FT-IR spectra of analyzed samples.

In terms of morphology, one can appreciate the fact that samples are different, even if results are grouped by class acoustic absorption. At sample 5 was determined that the pores are closed, with sizes between 200 and 600 μm . Pore wall thickness was measured between 20 and 50 μm . Sample 1 has a superior compactness than previous sample, but the determined presence of clusters (arising due to cracking) certainly created when cutting. Pore size is between 20 and 50 μm , and wall thickness between 5 and 10 μm . Pore shape is irregular, observing a slight elongation of the circular form. Sample 4 reveals an irregular shape of the pores with pore sizes much larger

than other samples. Pore diameter in this case is between 500 μm and 1mm and thickness of the walls between 10 and 20 μm . Imaging analysis revealed that the pore walls are fragile, leading to the separation of portions of the clusters. Sample 6 is completely different from other samples analyzed because do not have pores and consist only in fibrillar structure. Fiber length could not be determined, but it approximates the order of millimeters. The thickness of the fibers is also diverse, ranging in area from 20 to 60 μm . There was a significant compactness of the fibers, which are in intimate contact at a rate of about 50%. Sample 3 shows pores with irregular morphology,

slightly elongated longitudinally, open in approximately 50%. Pore size is between 100 and 400 μm and wall thickness between 5 and 15 μm .

Sample 2 is similar to previously analyzed sample, except that the pore shape is uneven but un-elongated. Their size was determined to be between 150 and 400 μm . It was observed that the pores are open at a rate of about 50%.

3. FT-IR analysis

The infrared analysis measures the type and intensity of molecular vibrations in the materials and gives important information related to molecular structure. The FT-IR spectra were performed using a Bruker Tesnor 27 instrument with diamond ATR annex and the acquisition was performed in "absorbance mode". The FT-IR spectra indicate that samples 2, 3 and 4 are commercially available polyester based materials with some small differences between them, which will be discussed. The large band at 2360 cm^{-1} is attributed to a large quantity of free water in the material porosity. It is interesting that the sample 3 does not present this amount of water, fact that suggest that the porosity does not permit this, or, more probable that the material is additivated with some hydrophobic substances that not allow the presence of free water molecules. The bands at 2849 cm^{-1} and 2917 cm^{-1} are attributed to $-\text{CH}_2$, respectively $-\text{CH}_3$ functional groups from polymeric chain structure. The variation of their intensity (which decrease in the following order: in sample 1 is more intense in comparison with sample 3, which is more intense in comparison with sample 2, in sample 4 being almost heavy detectable) gives information about chain length and also regarding the molecular weight of the polymer which decrease in order M (sample 1) $>$ M (sample 3) $>$ M (sample 2) $>$ M (sample 4). The absorption band at 1260 cm^{-1} is attributed in all samples to esteric functional group. The lower intensity of this band can be explained by the long length of polymer chain (usually, the commercially available polyesters for building applications present higher molecular weight) and also by the presence of additives in the material structure. The band present at 1733 cm^{-1} is attributed to $-\text{CO}$ functional group which proofs the polymer based polymer type. Other not very important bands can be observed at 1430-1470 cm^{-1} which indicates the stretching vibration of C-H bonds from CH, CH_2 and CH_3 functional groups, 1158 cm^{-1} which indicate the presence of $-\text{C}-\text{O}-\text{C}-$ in polyester and 1374 cm^{-1} which is specific for CH_2 geminal groups. In sample 3 we can observe a large band at 3200-3500 cm^{-1} which indicates the presence of an additive or other polymer compound with hydroxyl groups. Other bands can be attributed to different wastes, impurities or additives due to manufacturing process and due to the fact that the potential applications of these materials do not require high purity conditions.

The spectra performed for samples 5 and 6 indicate a compound based on polyester and polyurethane. The band

at 1507 cm^{-1} is attributed to $-\text{N}-\text{H}$ group from polyurethane structure and the bands from 3421-3446 cm^{-1} are also attributed to iminic groups from polyurethane. The other important bands were previously discussed for polyester. Both samples presents large quantity of free water (band at 2360 cm^{-1}) fact that suggests that the materials are to porous or that were not treated with hydrophobic agents. Samples 2, 3 and 5 present a very intensive band at 696 cm^{-1} which indicate the presence of a phosforylated additive with P-O-C functional group. These additives are usually used for building materials because they offer good thermal stability to the material and also the material became a good thermal and acoustic isolator.

4. Study of absorption and reflection coefficient by transfer function method

The sound pressure of the incident wave p_I and the reflected wave p_R are respectively:

$$p_I = \hat{p}_I e^{jk_0 x} \quad (1)$$

and

$$p_R = \hat{p}_R e^{-jk_0 x} \quad (2)$$

where \hat{p}_I and \hat{p}_R are the complex magnitudes of p_I and p_R at the reference plane ($x=0$) – see in Fig. 5. and $k_0 = k'_0 - jk''_0$ is the complex wave number, where k'_0 is the real component and k''_0 is the imaginary component which is the attenuation constant.

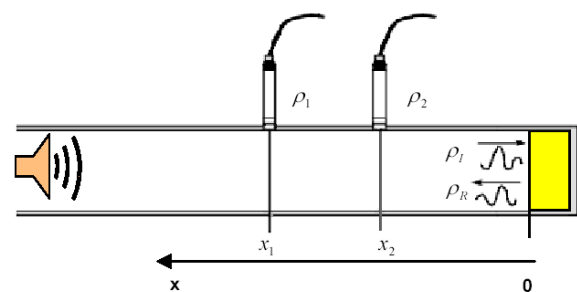


Fig. 4. The sound pressure of the incident and reflected wave.

In such short tube where no real attenuation can be measured, it can be expressed as follow:

$$k_0 \approx k'_0 = \frac{2\pi}{\lambda_0} = \frac{2\pi f}{c_0} = \frac{\omega}{c_0} \quad (3)$$

where

ω is the angular frequency

f is the frequency

c_0 is the speed of the sound equal to $343.2\sqrt{T/293}$ in m/s, where T is the temperature in Kelvin

The sound pressure p_1 and p_2 at the two microphones positions are:

$$p_1 = \hat{p}_I e^{jk_0 x_1} + \hat{p}_R e^{-jk_0 x_1} \quad (4)$$

and

$$p_2 = \hat{p}_I e^{jk_0 x_2} + \hat{p}_R e^{-jk_0 x_2} \quad (5)$$

The transfer function H_{12} for the total sound field between the two microphones may now be obtained by using equations (3) and (4) as follow:

$$H_{12} = \frac{p_2}{p_1} = \frac{\hat{p}_I e^{jk_0 x_2} + \hat{p}_R e^{-jk_0 x_2}}{\hat{p}_I e^{jk_0 x_1} + \hat{p}_R e^{-jk_0 x_1}} \quad (6)$$

The complex amplitude reflection factor r is the ratio of the complex amplitude of the reflected wave to that of the incident wave at the reference plane wave propagation (normal incidence):

$$r = \frac{p_R}{p_I} = \frac{\hat{p}_R e^{-jk_0 x}}{\hat{p}_I e^{jk_0 x}} = \frac{\hat{p}_R}{\hat{p}_I} e^{-2jk_0 x}$$

that can be simplified at $x = 0$ as

$$r = \frac{\hat{p}_R}{\hat{p}_I} \quad (7)$$

Therefore equation (11) can be expressed as follow:

$$H_{12} = \frac{p_2}{p_1} = \frac{\hat{p}_I e^{jk_0 x_2} + \hat{p}_R e^{-jk_0 x_2}}{\hat{p}_I e^{jk_0 x_1} + \hat{p}_R e^{-jk_0 x_1}} = \frac{e^{jk_0 x_2} + \frac{\hat{p}_R}{\hat{p}_I} e^{-jk_0 x_2}}{e^{jk_0 x_1} + \frac{\hat{p}_R}{\hat{p}_I} e^{-jk_0 x_1}} = \frac{e^{jk_0 x_2} + r e^{-jk_0 x_2}}{e^{jk_0 x_1} + r e^{-jk_0 x_1}} \quad \text{at } x = 0 \quad (8)$$

And transposing (7) to yield r at $x = 0$ as follow:

$$H_{12} (e^{jk_0 x_1} + r e^{-jk_0 x_1}) = e^{jk_0 x_2} + r e^{-jk_0 x_2} \Rightarrow$$

Then

$$H_{12} e^{jk_0 x_1} - e^{jk_0 x_2} = r e^{-jk_0 x_2} - H_{12} r e^{-jk_0 x_1} \Rightarrow$$

And then

$$r = \frac{H_{12} e^{jk_0 x_1} - e^{jk_0 x_2}}{e^{-jk_0 x_2} - H_{12} e^{-jk_0 x_1}} \quad (9)$$

This equation can be factorized as follows:

$$r = \frac{H_{12} - \frac{e^{jk_0 x_2}}{e^{jk_0 x_1}}}{\frac{e^{-jk_0 x_2}}{e^{-jk_0 x_1}} - H_{12}} \frac{e^{jk_0 x_1}}{e^{-jk_0 x_1}} = \frac{H_{12} - e^{-jk_0(x_1-x_2)}}{e^{jk_0(x_1-x_2)} - H_{12}} e^{2jk_0 x_1} = \frac{H_{12} - e^{-jk_0 s}}{e^{jk_0 s} - H_{12}} e^{2jk_0 x_1} \quad (10)$$

where $s = x_1 - x_2$ is the distance between the microphones.

The Complex amplitude reflection factor r at the reference plane ($x = 0$) can now be determined from the measured functions, the distance x_1 of the first microphone, the distance s between the microphones and the complex wave number k_0 which may include the tube attenuation constant k_0'' .

Sometimes equation (7) is expressed as follow:

$$r = \frac{H_{12} - H_I}{H_R - H_{12}} e^{2jk_0 x_1} \quad (11)$$

where

$$H_I = e^{-jk_0 s} = e^{-jk_0(x_1-x_2)} = \frac{e^{jk_0 x_2}}{e^{jk_0 x_1}} = \frac{\hat{p}_I e^{jk_0 x_2}}{\hat{p}_I e^{jk_0 x_1}} = \frac{p_{2I}}{p_{1I}} \quad (12)$$

this is the transfer function between the two microphones of the incident wave alone;

and

$$H_R = e^{jk_0 s} = e^{jk_0(x_1-x_2)} = \frac{e^{-jk_0 x_2}}{e^{-jk_0 x_1}} = \frac{\hat{p}_R e^{-jk_0 x_2}}{\hat{p}_R e^{-jk_0 x_1}} = \frac{p_{2R}}{p_{1R}} \quad (13)$$

this is the transfer function between the two microphones of the reflected wave alone.

Back to equation (10), the normal reflection factor r can be expressed as follow [8,9]:

$$r = \bar{r} e^{j\phi_r} = r_r + jr_i = \frac{H_{12} - H_I}{H_R - H_{12}} e^{2jk_0 x_1} \quad (14)$$

where

r_r is the real component;

r_i is the imaginary component;

ϕ_r is the phase angle of the normal incidence reflection factor.

From equation (10) or (13) the sound absorption coefficient will be calculated as follow [8-10]:

$$\alpha = 1 - |r|^2 = 1 - \sqrt{r_r^2 + r_i^2}^2 = 1 - r_r^2 - r_i^2 \quad (15)$$

assuming it equal to the Complex power transmitted factor

$$|r|^2 + \frac{Z}{\rho c_0} |t|^2 = 1.$$

The specific acoustic impedance ratio z called sometimes "Normalized impedance ratio" can be calculated from (10) or (13) as follow:

$$z = \frac{Z}{\rho c_0} = \frac{R}{\rho c_0} + j \frac{X}{\rho c_0} = \frac{(1+r)}{(1-r)} \quad (16)$$

where

Z is the normal sound incidence impedance defined as follow:

$$Z = \frac{p}{u}$$

where

p is the sound pressure at the reference plane ($x = 0$);

u is the sound particle velocity at the reference plane ($x = 0$);

and for plane wave propagation (normal incidence).

Upper working frequency (f_u) limited by:

- The cross section of the tube
 $d < 0.58 * \lambda_u \Rightarrow f_u < 0.58 * c_0 / d$ (Circular tube) (ISO 10534-2)
- The spacing between the microphones
 $s < 0.45 * \lambda_u \Rightarrow f_u < 0.45 * c_0 / s$ (ISO 10534-2)

The upper working frequency is chosen to avoid the occurrence of non-plane wave mode propagation and to assure accurate phase detection.

f_u : upper working frequency [Hz]

d : inside diameter of circular tube [m]

s : spacing between microphones [m]

c_0 : speed of sound [m/s]

To determine the acoustic absorption coefficient of acoustic interferometer method -Kundt tube was used. Method for determining the absorption characteristic is in accordance with applicable European standards SR EN ISO 10534-1:2002 and SR EN ISO 10534-2:2002 [12,13].

The test apparatus consists of an acoustic interferometer tube type 4206-A (the average tube), a signal acquisition system simultaneously on five channels with signal generator - PULSE analyzer platform type 3560-B-030, two microphones, type 4187, amplifier signal acoustic calibrator type 2716 and 4231 DP-0775 adapter for earphones, all these instruments are manufactured by Brüel & Kjær. Frequency domain tested for absorption curves of the acoustic interferometer type 4206 A is between 100 Hz and 3.2 kHz.

For registration and automatic processing of signals from the two microphones using a PC computer system

(laptop) that has installed a 7758-type analysis software - PULSE Material Testing, which is part of the package PULSE Ver. 12.5, Brüel & Kjær. To characterize the environment in which sound absorption determinations are made, especially for precise identification of the speed of sound in air, are measured: air pressure, temperature and relative humidity.

It was determined the input parameters for measuring equipment, respectively the atmospheric pressure 1033 hPa, the medium temperature of 28.00 °C and relative humidity of 56%, then these features were automatically calculated: velocity of sound is 347.89 m/s, density of air is 1.193 kg/ m³ and impedance characteristic of air 415.0 Pa/(m/s).

In this case we have: microphone spacing of 0.0318 m, diameter of 0.0635 m, random waveform produced by a generator with 1.414 Vrms signal level. Sample thickness was: 4 mm for sample 1; 3 mm for sample 2 and 3; 15 mm for sample 4 and 5; 18 mm for sample 6.

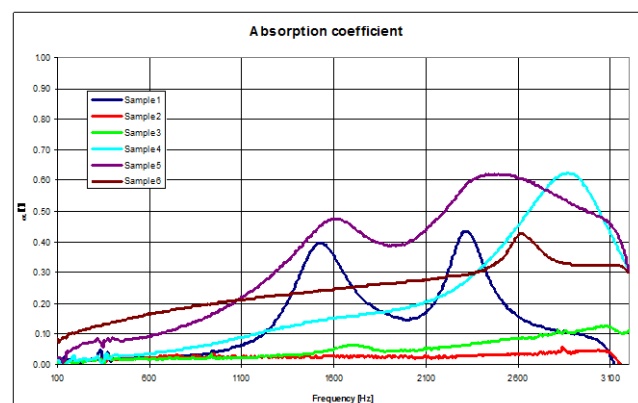


Fig. 5. Absorption coefficient for the analyzed samples.

The sound absorption coefficient indicates how much of the sound is absorbed in the actual material and varied in accordance with frequency. In Fig. 6 is presented the variation of sound absorption coefficient with frequency, in case of different materials.

The sample 4, 5 and 6 are characterized by high absorption for frequency range between 1500 – 3200 Hz. The sample 1 have a relative high absorption coefficient, with mention that the range of frequency from 1200 - 2500 Hz, and we can see two peaks corresponding to some common resonance at around of 1500 Hz and 2300 Hz. Also, a low absorption is observed for samples 2 and 3.

Following these tests, it can be noticed that the porosity and composition of materials analyzed in previous chapter's influences the sound absorption and reflection.

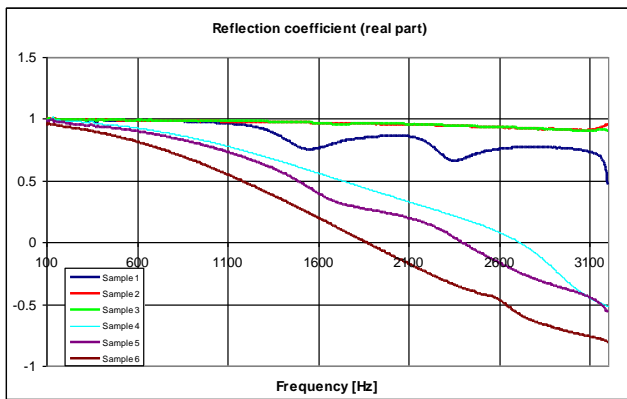


Fig. 6. Reflection coefficient (real part) for the analyzed samples.

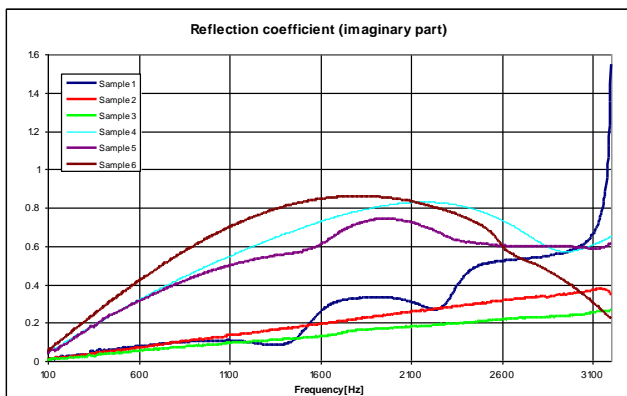


Fig. 7. Reflection coefficient (imaginary part) for the analyzed samples.

In Figs. 6 and 7 corresponding experimental results are presented separately the real part and imaginary part of the reflection coefficient. These graphs highlight the clear variation of the two coefficients r_r and arising r_i in relation (14).



Fig. 8. Reflection coefficient $|r|$ for the analyzed samples.

According to these coefficients r_r and r_i , result the reflection coefficient module $|r|$, which is shown in Figure 8 for the all studied samples. In this figure it can be seen easily from the reflection coefficient dependence of absorption coefficient, this dependence is shown above in equation (15). The sample 4, 5 and 6 are characterized by low reflection for frequency range between 1500 – 3200 Hz. The sample 1 have a relative low reflection coefficient, with mention that the range of frequency from 1200 - 2500 Hz, in the same way as the absorption coefficient from Fig. 6, we can see two peaks corresponding to some common resonance at around of 1500 Hz and 2300 Hz. Also, a high reflection is observed for samples 2 and 3 where values of over 0.95 on almost the entire frequency range considered.

4. Conclusions

Sound absorption and reflection is one of the most important acoustical properties which characterized the porous materials used in construction with sound insulation role as sound barriers or interior floors and walls of the buildings.

Following these multiple tests, we can say that materials such as samples 2 and 3 can only be used for acoustic insulation. In the same vein, appropriate material samples 1, 4, 5 and 6 can be used as needed for acoustic absorption. Also on the acoustic characteristics of absorption and reflection of the 6 samples has their thickness, so that for these types of materials increases as the thickness, increases the absorption coefficient and thus reflection coefficient is reduced. It also can be seen that the pore size, link-correlation between the pore and chemical composition of materials studied have a significant influence on the absorption properties. If a high percentage of pores are closed and the material has a smaller thickness the absorption curve decreases.

After microscopic analysis to highlight the structure and pores size of the material, FT-IR analysis of the chemical composition of materials and finally the analysis of acoustic point of view, we can see that they are closely related. Porosity and composition of materials for the six samples analyzed affect sound absorption feature and reflection.

In the future, the authors aim to analyze this combined correlation for other types of materials, which may be a clearer and more obvious difference.

Acknowledgment

The authors acknowledge the support of the Managing Authority for Sectorial Operational Programme for Human Resources Development (AMPOSDRU) for creating the possibility to perform these researches by Grant POSDRU/89/1.5/S/62557.

References

- [1] A. C. Nechifor, M. G. Stoian, S. I. Voicu, G. Nechifor, *Optoelectron. Adv. Mater. – Rapid Commun.* **4**(8), 1118 (2010).
- [2] C. Baicea, A. C. Nechifor, D. I. Vaireanu, O. Gales, R. Trusca, S. I. Voicu, *Optoelectron. Adv. Mater. – Rapid Commun.* **5**(11), 1181 (2011).
- [3] Online edition for students of organic chemistry lab courses at the University of Colorado, Boulder, Dept of Chem and Biochem, 155 (2002).
- [4] F. D. Balacianu, A. C. Nechifor, R. Bartos, S. I. Voicu, G. Nechifor, *Optoelectron. Adv. Mater. – Rapid Commun.* **3**(3), 219 (2009).
- [5] S. I. Voicu, A. C. Nechifor, B. Serban, G. Nechifor, M. Miculescu, J. *Optoelectron. Adv. Mater.* **9**(11), 3423 (2007).
- [6] M. Bratu, I. Ropotă, O. Vasile, O. Dumitrescu, M. Muntean, *Romanian Journal of Materials* **41**(2), 147-154 (2011).
- [7] P. Bratu, N. Dragan, O. Vasile, The 11-th International Congress on Automotive and Transport Engineering CONAT 2010, Proceedings – Volume III "Automotive Vehicles and Environment", 177-184 (2011).
- [8] M. D. Stanciu, N. Cretu, C. Rosca, I. Curtu, *Romanian Journal of Acoustic and Vibration* **V**(1), 3-10 (2008).
- [9] S. J. Sung, T. K. Yong, B. L. Yong, *Journal of Korean Physical Society* **53**(2), 596 (2008).
- [10] O. Vasile, Annual Symposium of the Institute of Solid Mechanics and Session of the Commission of Acoustics, SISOM 2011, 25-26 May 2011, Bucharest, Romania.
- [11] C. Cosereanu, C. Lazarescu, I. Curtu, D. Lica, D. Sova, L. Brenci, M. D. Stanciu, *Rev. Materiale Plastice*, **47**(3), 341 (2010)
- [12] ISO 10534-1:2002 Acoustics – Determination of sound absorption coefficient and impedance in impedance tubes – Part 1: Method using standing wave ratio.
- [13] ISO 10534-2:2002 Acoustics – Determination of sound absorption coefficient and impedance in impedance tubes – Part 1: Transfer-function method.
- [14] G. Nechifor, S. I. Voicu, A. C. Nechifor, G. Nechifor, *Desalination* **241**, 342 (2009).
- [15] V. I. Luntraru, O. Gales, L. Iarca, E. Vasile, S. I. Voicu, A. C. Nechifor, *Optoelectron. Adv. Mater. – Rapid Commun.* **5**(11), 1229 (2011).

*Corresponding author: ovidiu_vasile2002@yahoo.co.uk